HHS Public Access

Author manuscript

Osteoarthritis Cartilage. Author manuscript; available in PMC 2017 December 12.

Published in final edited form as:

Osteoarthritis Cartilage. 2017 July ; 25(7): 1143–1149. doi:10.1016/j.joca.2017.03.001.

Reinforcement of Articular Cartilage with a Tissue-interpenetrating Polymer Network Reduces Friction and Modulates Interstitial Fluid Load Support

Benjamin G. Cooper[1,2], **Taylor Lawson**[2,3], **Brian D. Snyder**[2,4,5,*], and **Mark W. Grinstaff**[1,4,*]

[1]Department of Chemistry, Boston University, Boston, Massachusetts, United States

[2]Center for Advanced Orthopaedic Studies, Beth Israel Deaconess Medical Center, Harvard Medical School, Boston, Massachusetts, United States

[3]Department of Mechanical Engineering, Boston University, Boston, Massachusetts, United States

[4]Departments of Biomedical Engineering and Medicine, Boston University, Boston, Massachusetts, United States

[5]Department of Orthopaedic Surgery, Boston Children's Hospital, Boston, Massachusetts, United States

Abstract

Objective—Osteoarthritis is associated with increased articular cartilage hydraulic permeability and decreased maintenance of high interstitial fluid load support during articulation, resulting in increased friction on the cartilage solid matrix. This study assesses frictional response following *in situ* synthesis of an interpenetrating polymer network designed to mimic glycosaminoglycans depleted during osteoarthritis.

Methods—Cylindrical osteochondral explants containing various interpenetrating polymer concentrations were subjected to a torsional friction test under unconfined creep compression. Time-varying coefficient of friction, compressive engineering strain, and interstitial fluid load support proportion were calculated and analyzed.

Results—The polymer network reduced friction coefficient over the duration of the friction test, both under moderate fluid load support as well as under 0% fluid load support. A positive trend was observed relating polymer network concentration with magnitude of friction reduction

*Corresponding author: Mark W. Grinstaff, PhD, Departments of Chemistry, Biomedical Engineering, and Medicine, Boston University, Boston, MA 02215, USA. Tel: 617-358-3429; mgrin@bu.edu. and Brian D. Snyder, PhD, MD Department of Orthopaedic Surgery, Boston Children's Hospital, Boston, Massachusetts, United States Brian.Snyder@childrens.harvard.edu.

Contributions

The manuscript was written through contributions of all authors. All authors have given approval to the final version of the manuscript.
BGC contributed to the study design, data acquisition and interpretation, manuscript drafting, and critical manuscript revision.
TL contributed to the data acquisition and interpretation and critical manuscript revision.
BDS contributed to the data interpretation and critical manuscript revision.
MWG contributed to the data interpretation, manuscript drafting, and critical manuscript revision, and takes responsibility for the integrity of the work's entirety (contact: mgrin@bu.edu).

Competing interest statement

None

compared to non-treated tissue. The calculated hydraulic permeability of polymer-treated tissue was 27% decreased compared to non-treated tissue.

Conclusion—The cartilage-interpenetrating polymer treatment improves lubrication by augmenting the biphasic tissue's interstitial fluid phase, and additionally improves the friction dissipation of the tissue's solid matrix. This technique demonstrates potential as a therapy to restore optimal tribological function of degenerated cartilage.

Keywords

Articular cartilage; Friction; Biolubrication; Biomaterials; Tissue reinforcement

INTRODUCTION

Articular cartilage is the smooth, hydrated hyaline cartilage that supports compressive and shear forces applied to diarthrodial joint surfaces, providing low coefficients of friction (COF) and resisting material failure for many decades of use in healthy individuals. Several general models for articular cartilage are described, including a biphasic framework (with tissue comprised of a *solid matrix* and an *interstitial fluid phase)* and a triphasic framework (incorporating an *ionic phase* of fixed and mobile charges). The *solid matrix* is comprised of an extracellular biopolymer matrix of predominantly type II collagen, along with hyaluronan, proteoglycan complexes (glycosaminoglycan (GAG) chains attached to a peptide backbone), and chondrocytes. Porosity and hence permeability of the solid matrix are key defining characteristics of this phase,[1] as are various other elements of structure including compressibility, anisotropy due to collagen fibril orientation,[2] and tensile strength of the matrix.[3] An aqueous solution of proteins, hyaluronan, and other solutes, known as synovial fluid, constitutes the tissue's *interstitial fluid phase*. As typically 65–85 w/w% of cartilage is water, the fluid phase plays an important physiologic role with respect to diffusion-based transport, and it also contributes significantly to tissue compressive properties. As cartilage is compressed, water (being incompressible) is expelled from the tissue; the rate of this expulsion is limited largely by the solid matrix's permeability, as well as by the GAGs which attract and retard the outward flow of water molecules. Thus, when the tissue is initially loaded in compression, nearly 100% of the load is supported by the fluid phase, and as water molecules flow out of the matrix as the tissue creeps to equilibrium under constant compressive load, the interstitial fluid load support (IFLS) decreases from near 100% to 0%.[4] Over this transition, the proportion of total load supported by the tissue's solid phase likewise increases from near 0% to 100% upon compressive equilibration. In a configuration of migrating rather than stationary loading contact, such as in various reciprocating friction testing experiments, IFLS may be maintained at a high value near 100% pending certain conditions, *e.g.* a substantially high ratio of time unloaded to time loaded, or a substantially low compressive force.[5] It should be noted that not all water molecules are mobile, and only "free" water in the fluid phase is able to exude from the tissue upon compression while "bound" water is electrostatically immobilized by fixed charges within the tissue[6] (hence "bound" water is more accurately classified as part of the solid phase than the fluid phase). The *ionic phase* of the tissue plays a role in triphasic theory of cartilage material and mechanical properties; fixed negative charges within the

solid matrix, arising from sulfate and carboxylate functional groups of GAGs, are balanced by mobile sodium, potassium, and calcium cations through Donnan equilibrium, and exhibit an electrostatic resistance to being compressed as the anionic groups repel one another upon loading.[7] Furthermore, the ionic phase gives rise to cartilage's dependence of compressive properties on salt concentration, with increasing presence of salts causing a charge screening effect and thereby decreasing the fixed negative charges' i) electrostatic resistance to compression and ii) attraction to mobile and non-mobile water molecules.[8]

As human knee and hip articular cartilage experiences about 1 million articulation cycles in a typical year, its lubrication is essential in maintaining low friction and wear. Owing to the biphasic nature of cartilage as well as its viscoelasticity and variability in loading conditions under different physiologic circumstances (*e.g.* alterations in synovial fluid viscosity with aging or disease, and various loading magnitudes caused by body weight and carrying load), several lubrication mechanisms have been proposed over the last half century.[4, 9–12] The majority of investigations of cartilage COF have been conducted at equilibrium (either in creep or stress-relaxation), when the IFLS is ~0%.[12–14] Under such conditions when nearly 100% of the load is supported by the tissue's solid phase, lubrication of cartilage is approximated as occurring analogous to that of a monophasic elastic solid, with classical modes of *boundary* and elastohydrodynamic (*fluid film*) lubrication being operative. An alternative mechanism, known as "*boosted*" lubrication, occurs as water molecules in the interposed fluid film between apposing cartilage surfaces are driven into the tissue matrix; this causes the local concentration of lubricating macromolecules in synovial fluid (hyaluronic acid, lubricin, and phospholipids) to be increased or "boosted," forming a lubricious gel at the tissue interface. In contrast to a 0% IFLS scenario, the presence of substantial IFLS greatly reduces the tissue's friction and causes alternate stress dissipation phenomena. Upon initial compressive loading concurrent with sliding, negligible solid-solid frictional forces exist between the apposing cartilage surfaces, since the tissue's interstitial fluid phase supports nearly 100% of the applied load. Under these ~100% IFLS conditions, the expulsion of interstitial fluid from the tissue's bulk and into the interfacial region between the tissues, known as "*weeping*," allows the two surfaces to be kept apart via a self-pressurized interfacial fluid in a hydrostatic mode of lubrication.[10, 15, 16] In these types of studies, the COF (as well as the creep deformation) varies directly with the IFLS,[4, 17, 18] and the ability to maintain near 100% IFLS has been postulated as a characteristic critical for affording low COF and high wear resistance over a synovial joint's many decades of use.

A primary disease of articular cartilage occurring with advanced age is osteoarthritis (OA), associated with degradation of cartilage material properties and causing wear. Consequently, significant research activities are directed at treating, augmenting, or repairing degraded cartilage[19–23] including, for example, polymer scaffolds for filling tissue defects,[24–28] lubricants for improving tribological properties,[29, 30] stimulating growth factors for promoting healing,[31] cell transplantation,[32, 33] and gene therapy for restoring biological activity.[34] An early hallmark of OA is the loss of GAGs with a resultant decrease in the dynamic and equilibrium compressive moduli of the cartilage by allowing increased rate of water exudation and decreased quantity of GAG-bound water, respectively. Furthermore, the hydraulic permeability of cartilage is increased, causing IFLS to decrease at a faster rate

upon loading, exacerbating cartilage degeneration by increasing the occurrence of solid-solid contact-derived friction.[35]

Currently, there are no therapies that mitigate the loss of GAGs or effectively replace lost GAGs. We hypothesize that a treatment which restores high IFLS may improve cartilage function by reducing solid-solid interfacial friction. We recently reported a new cartilage-reinforcing technique—administration of a GAG-inspired zwitterionic polymer 2-methacryloyloxyethyl phosphorylcholine (pMPC) that reconstitutes cartilage matrix hydrophilicity.[36] The treatment involves forming, through *in-situ* photopolymerization, a semi-synthetic interpenetrating polymer network (IPN) entangled with native collagen fibrils (Figure 1a) that increases the compressive stiffness and wear resistance of treated cartilage during accelerated wear testing against stainless steel when IFLS began high and was allowed to subside. The present study investigates the frictional response of IPN-treated cartilage sliding against IPN-treated cartilage and the effects of the interpenetrating polymer on the relationship between normalized strain values ($\varepsilon/\varepsilon_{eq}$) and COF.

METHODS

Sample preparation and IPN treatment

Nine pairs of osteochondral cylindrical plugs (7 mm diameter, cartilage thickness ranging approximately 1–1.5 mm) were cored from the stifle joints of skeletally mature cows in a procedure similar to those reported previously[12, 37] using a diamond-tipped coring bit (Starlite Industries, Bryn Mawr, PA), irrigated with 0.9% saline at room temperature. Throughout experimentation, plugs were stored at 4°C in 400 mOsm sodium chloride solution containing protease inhibitor benzamidine hydrochloride (5 mM), GIBCO Antibiotic/Antimycotic (Invitrogen, Grand Island, NY), and calcium ion chelating agent ethylenediamine tetraacetic acid (5 mM). The nine plug pairs were randomly sorted into three groups of N=3 pairs. Two groups of N=3 osteochondral plugs were incubated in the dark for 24 h at 25°C in 400 mOsm saline containing 2-methacryloyloxyethyl phosphorylcholine (either 20 or 60 w/v%), ethylene glycol dimethacrylate (1% mol/mol 2-methacryloyloxyethyl phosphorylcholine), eosin Y (0.1 mM), triethanolamine (115 mM), and N-vinylpyrrolidone (94 mM). Plugs were suspended upside down with articular surface exposed to solution to allow diffusion of solutes. Plugs were removed from solution, gently blotted dry with paper towel, and irradiated with green light (514 nm) at 500 mW/cm^2 for 10 min (Ultima SE, Lumenis, Santa Clara, CA). Photoirradiation was performed in a humid chamber to prevent tissue drying. Plugs were then rinsed in saline to allow residual non-reacted monomer and photoinitiator to wash out.

Friction testing

Specimens (non-IPN treated native cartilage or cartilage treated with IPN at a monomer concentration of 20 or 60 w/v%, N=3 each) were subjected to a torsional disc-on-disc unconfined friction test, lubricated by 400 mOsm saline (Figure 1b). The procedure was composed of simultaneous constant compressive stress (0.78 MPa) and torsion (10,080 rotations, 360° s^{-1}, effective perimeter velocity 22 mm s^{-1}; 10-s lift-offs every 160 s to allow saline lubricant reintroduction to the tissue interface) (TA Electroforce 3200). The

instantaneous creep deformation was measured over time and converted to compressive engineering strain given the known cartilage thickness determined via average caliper measurement at six locations around each plug's circumference. COF was calculated from the torque and normal force measured at 10 Hz. Both creep deformation and COF values were binned and averaged over sequential 160-s intervals.

Estimation of IFLS

IFLS has been measured directly in prior reports using a microchip piezoresistive pressure transducer placed on face of cylindrical cartilage discs opposite the articular surface (separated from subchondral bone with a sledge microtome),[3, 38, 39] and creep deformation has been theorized[40, 41] and experimentally demonstrated[17] to linearly correlate with IFLS. In the present study, IFLS is not measured directly but rather is inferred from the value of instantaneous compressive engineering strain normalized by equilibrium compressive engineering strain, $\varepsilon/\varepsilon_{eq}$. IFLS values were thus approximated, ranging from 100% at the beginning of the test when $\varepsilon/\varepsilon_{eq}$ = 0%, and subsiding towards 0% as $\varepsilon/\varepsilon_{eq}$ equilibrated at 100%,. $\varepsilon/\varepsilon_{eq}$ values were binned and averaged over sequential 160-s intervals.

Statistics

Statistically significant differences in COF and ε were identified via Student's t-tests with two-tailed probability level $p < 0.05$. In comparing the time-dependent COF and time-dependent ε of treatment groups with the non-treatment group, repeated pair-wise t-tests were performed at each time point. Similarly, comparisons of ε-dependent COF of treatment groups and non-treated group were performed by repeated pair-wise t-tests at each $\varepsilon/\varepsilon_{eq}$ value.

RESULTS

Over the duration of the three-hour torsional friction test, COF increased as a function of time for non-IPN treated cartilage as well as for both groups of IPN-treated cartilage containing 20 and 60 w/v% interpenetrating polymer (Figure 2). A statistically significantly lower COF was observed for the 60 w/v% IPN treated plugs compared to the non-IPN treated plugs after 4960 seconds of the 10,080-second test elapsed. The equilibrium COF, upon the test's completion (COF_{eq}), was 24% less (95% confidence interval 14–34% less) than that of non-treated tissue ($p = 0.015$). The COF of the 20 w/v% treated plugs did not statistically significantly differ from that of non-treated plugs ($p = 0.48$, 95% confidence interval −7 to 18% less than that of non-treated tissue).

The creep deformation, represented as the compressive engineering strain ε, also increased as a function of time for all three treatment groups (Figure 3). ε became statistically significantly different between non-treated and 60 w/v% treated groups after 320 seconds, with equilibrium strain (ε_{eq}) 22% less (95% confidence interval 16 to 29% less) for 60 w/v% treated tissue than for that of non-treated tissue ($p = 0.022$). The 20 w/v% treated tissue and non-treated tissue did not statistically significantly differ in instantaneous ε, nor in ε_{eq} (for ε_{eq}, $p = 0.82$, 95% confidence interval −20 to 24% less than that of non-treated tissue). The creep equilibration time constant τ_{ε} (*i.e.,* the characteristic time constant required for ε to

rise ($1\text{-}e^{-1}$) percent of the way towards ε_{eq}) increased non-statistically significantly ($p = 0.33$) by 9% for the 60 w/v% treated compared to non-treated tissue (time constant 1233 ± 29 vs 1133 ± 153 seconds, means ± standard deviations).

Normalized compressive strain, $\varepsilon/\varepsilon_{eq}$, increased from approximately 40% averaged over the test's first 160 s, to 100% upon the test's completion. The COF was plotted as a function of $\varepsilon/\varepsilon_{eq}$, revealing distinct relationships for each treatment group, each fit with a least squares exponential regression curve ($R^2 > 0.995$) (Figure 4). For both concentrations of IPN treatment, percent reduction in COF compared to COF of non-treated tissue was calculated and plotted as a function of $\varepsilon/\varepsilon_{eq}$; both groups demonstrate greater reductions at greater $\varepsilon/\varepsilon_{eq}$ values, with the 60 w/v% IPN treated group's COF being statistically significantly lower than that of the non-treated group ($p < 0.05$) for $\varepsilon/\varepsilon_{eq}$ values ≥ 94% (Figure 5). The reduction in COF for the 20 w/v% IPN treatment group was not statistically significant over the range of $\varepsilon/\varepsilon_{eq}$ studied.

DISCUSSION

In a frictional creep test of the nature performed in this study, the COF is interrogated as IFLS begins at 100% and subsides. A creep stress of 0.78 MPa was selected to mimic the contact stresses experienced in the knee during jogging,[42] and effective perimeter velocity of 22 mm s^{-1} was selected to mimic the upper physiologic range of daily femoral-tibial sliding velocities.[43] This procedure yields COFs that increase as a function of time[44] as shown in Figure 2, with COFs equilibrating concurrent with creep deformation equilibrium. The differences in COF became statistically significant between 60 w/v% treated and non-treated tissue approximately half-way into the three-hour test (24% reduction in COF compared to non-treated tissue at the test's completion), whereas the difference in COF between 20 w/v% and non-treated tissue demonstrated a non-statistically significant ($p = 0.48$) 5% reduction in COF compared to non-treated tissue. The IPN dose-dependence of the frictional response agrees with the observed dose-dependence of the compressive stiffness and wear-resistance as reported in our prior study,[36] and the IPN's reduction of friction reported herein may be one of the primary reasons causing its improvement in wear-resistance. While the magnitude of COF is affected by the presence of IPN, the characteristic shapes of the three COF curves as a function of time are not statistically significant; all three curves possess similar COF equilibration time constants.

Engineering compressive strain ε statistically significantly differed as a function of time over the majority of the friction test for the 60 w/v% treated tissue compared with non-treated tissue (Figure 3). This attenuation of creep deformation (22% reduction by the test's equilibrium) is related to the increased equilibrium stiffness that the IPN imparts.[36] Similar to the COF vs time profiles, the creep deformation time profiles do not statistically significantly differ in equilibration time constant τ_ε ($p = 0.33$), with τ_ε lengthened by 9% for the 60 w/v% treated compared to non-treated tissue. This increased time constant represents the increased time required for tissue to deform in response to the constant load applied, and likely originates from two underlying mechanisms. First, the IPN's retardation of water's expulsion from the tissue occurs due to the polymer network's highly hydrophilic functional groups' attraction to flowing water molecules, hence slowing their flow, as well as the

polymer network's effective decrease in the tissue's hydraulic permeability due to physical occupation of tissue pores, thus decreasing the effective pore size. Indeed, an effective hydraulic permeability κ may be calculated[45, 46] given sample thickness h and h_{eq} in initial and equilibrium compressed state, respectively, creep deformation equilibrium time constant τ_ε, and equilibrium compressive modulus E (calculated from the ratio of equilibrium stress to equilibrium strain) from Equation 1,

$$\kappa = \frac{h h_{eq}}{\pi^2 \tau_\varepsilon E} \quad (1)$$

The non-treated tissue's time constant of 1133 ± 153 seconds is found to correspond to a calculated hydraulic permeability of $3.4 \cdot 10^{-16}$ $m^2/Pa \cdot s$, while the 60 w/v% treated tissue's 9% increased time constant of 1233 ± 29 corresponds to a 27% decreased calculated hydraulic permeability of $2.4 \cdot 10^{-16}$ $m^2/Pa \cdot s$; this phenomenon represents an augmentation of the tissue's fluid phase in that decreased permeability is associated with a longer duration of sustained fluid load support.[35] Hydraulic permeability values ranging $1 \cdot 10^{-16}$-$1 \cdot 10^{-14}$ $m^2/Pa \cdot s$ are typical of bovine articular cartilage.[47–49] The second mechanism explaining the lengthened time constant value upon IPN treatment is the entropic contribution from the interpenetrating polymer network, as the relatively mobile polymer chains occupy a variety of conformational states during the process of matrix compressive equilibration, thus increasing the time required for deformation to equilibrate under constant stress. Unlike a change in the matrix's hydraulic permeability, the entropic contribution of the polymer to creep relaxation represents a change in fluid-flow-*independent* viscoelasticity of the solid phase, and the two described mechanisms together indicate that the IPN may directly influence both the solid phase and the fluid phase of the tissue.

$\varepsilon/\varepsilon_{eq}$ varied similarly with time for all three treatment groups. We hypothesized that increasing concentrations of IPN, particularly at 60 w/v%, would sustain elevated IFLS values over the beginning portion of the test, effectively enabling the tissue's fluid phase to support a greater proportion of load (compared to the solid matrix's load support), as well as maintain the elevated load support for a longer duration than non-IPN-treated tissue. This finding was not observed, as non-treated and 60 w/v% IPN treated tissue demonstrated similar $\varepsilon/\varepsilon_{eq}$ time course profiles (reflective of IFLS).

The lack of significant difference between the normalized strain values $\varepsilon/\varepsilon_{eq}$ of the groups may derive from the inherent difference in their magnitude of creep deformation, and the existence of an intimate connection between the equilibrium compressive deformation ε_{eq} and the rate at which the deformation occurs. In particular, there exist maximum confining limits on the phenomena that govern the rate of tissue deformation under compressive load, including i) rate of bound or interstitial water dissociating from nearby charged or otherwise hydrophilic centers and becoming free or bulk water, ii) velocity of water molecules exuding through the tissue matrix (limited by permeability), and iii) rate of solid biopolymer matrix collapse and rearrangement. Each of these types of events, along with possible others, possess probabilistically maximum rates at which they occur, which, when summed together, govern an upper bound to the rate at which articular cartilage can compress under

load. In the present study, both the non-treated tissue and 60 w/v% treated tissue were initially loaded with identical stress and began compressing at similar deformation rates, yet the non-treated tissue's ε_{eq} was significantly greater than the 60 w/v% treated tissue's ε_{eq} (43% vs 33%). Thus, it follows that the non-treated tissue's IFLS cannot simply decrease as rapidly as hypothesized, since the upper limit of the calculated IFLS is confined by the maximal rates of tissue deformation. To address this, future studies of this tissue treatment technique will investigate differences in creep time course profiles and directly-measured IFLS time course profiles for tissues with equivalent equilibrium deformations, to rule out convoluting effects of this variable.

Finally, we examined the IPN's effect on the relationship between COF and $\varepsilon/\varepsilon_{eq}$. Whereas COF's IPN dose dependence is not readily observed as a function of time (Figure 2), a clear trend is apparent in COF as a function of $\varepsilon/\varepsilon_{eq}$; for any particular normalized strain value (reflecting IFLS), increasing IPN concentrations provide reduced COF (Figure 5) This indicates that the IPN's presence alters the frictional response of the tissue. Given that, at greater $\varepsilon/\varepsilon_{eq}$ values, equivalent COFs can be attained when increasing IPN concentrations are present, the IPN may enable articular cartilage to be loaded with greater force (*e.g.* increased body weight or carrying load) while still allowing equivalent COF to non-treated tissue without the additional load.

Percent reduction in COF of IPN treated tissue compared to that of non-treated tissue reveals not only that 60 w/v% IPN provides improved lubrication compared with 20 w/v%, but also that the magnitude of improvement is further increased at greater $\varepsilon/\varepsilon_{eq}$ (statistically significantly so for $\varepsilon/\varepsilon_{eq} \geq 94\%$ (Figure 5). When IFLS is low and solid matrix load support is high, cartilage behaves more similarly to a classical monophasic elastic material under friction; under such conditions, along with the low lubricant viscosity (ca. 1 mPa·s), moderate speed (22 mm s^{-1}), and moderate stress (0.78 MPa) of the testing configuration, boundary mode lubrication operates.[5] The IPN's reduction of friction under equilibrium, boundary lubrication conditions indicates that the tissue-interpenetrating polymer network either i) continues to assist either the solid or fluid phase of the tissue dissipate frictional forces, or ii) a certain amount of surface-active polymer contributes directly to friction dissipation as a boundary lubricant. These possibilities warrant further investigation by directly measuring the IFLS at creep-equilibrium and by grafting the GAG-inspired zwitterionic polymer to the articular surface without penetrating the bulk, respectively.

The scope of this study is limited in that compressive and frictional properties are heavily dependent upon loading and operating conditions; interpretations of the results apply specifically to the load, rotational speed, specimen geometry, and lubricant used in this experiment. Unconfined compression used in the present study allows lateral exudation of water through non-physiologic cut edges around the plug's circumference; the IPN's ability to alter interstitial fluid flow should be examined in unconfined plug compression or in an intact joint surface model. Two IPN concentrations were studied; investigation of concentrations between 20 and 60 w/v% and also greater than 60 w/v% are underway. Alternate loads, as well as articulation speeds and lubricant types, should be investigated to further understand the IPN's effect on lubricating. Finally, this pilot study was conducted

with a sample size of three specimens per group, and future tests will be conducted to gain increased statistical power.

CONCLUSION

In summary, the reinforcement of articular cartilage with a GAG-inspired interpenetrating polymer network reduces the tissue's time-varying COF under both high and low IFLS conditions. The IPN mechanically mimics the ability of matrix-localized GAG biopolymers to confer tissue lubrication as IFLS subsides from 100% towards 0%, and likewise reduces tissue hydraulic permeability. As both COF and hydraulic permeability increase with advancing osteoarthritis, the treatment technique investigated herein may restore tribological function of degenerated tissue to optimal levels. In the presence of IPN, the COF values reduce over a wide range of IFLS values, suggesting that the polymer network assists the fluid phase's dissipation of frictional forces and may in turn prevent physiologic wear by maintaining low friction. Continued development and evaluation of novel cartilage reinforcement therapies, such as this one as well as others, is encouraged, as it may yield additional treatment options beyond pain management and total joint replacement.

Supplementary Material

Refer to Web version on PubMed Central for supplementary material.

Acknowledgments

Funding Sources

This content was supported in part by the Harvard Catalyst Program and a National Science Foundation Graduate Research Fellowship under Grant No. DGE-1247312 (B.G.C.) and NIH Training Grant in Translational Biomaterials (T32EB006359).

The authors thank Boston University and Beth Israel Deaconess Medical Center for campus wide resources and institutional support.

References

1. Maroudas A. Biophysical chemistry of cartilaginous tissues with special reference to solute and fluid transport. Biorheology. 1975; 12:233–248. [PubMed: 1106795]
2. Chahine NO, Wang CCB, Hung CT, Ateshian GA. Anisotropic strain-dependent material properties of bovine articular cartilage in the transitional range from tension to compression. Journal of Biomechanics. 2004; 37:1251–1261. [PubMed: 15212931]
3. Soltz MA, Ateshian GA. A conewise linear elasticity mixture model for the analysis of tension-compression nonlinearity in articular cartilage. Journal of Biomechanical Engineering-Transactions of the Asme. 2000; 122:576–586.
4. Ateshian GA. The role of interstitial fluid pressurization in articular cartilage lubrication. Journal of Biomechanics. 2009; 42:1163–1176. [PubMed: 19464689]
5. Accardi MA, Dini D, Cann PM. Experimental and numerical investigation of the behaviour of articular cartilage under shear loading-Interstitial fluid pressurisation and lubrication mechanisms. Tribology International. 2011; 44:565–578.
6. Maroudas A, Schneiderman R. Free and exchangeable or trapped and non-exchangeable water in cartilage. Journal of Orthopaedic Research. 1987; 5:133–138. [PubMed: 3819905]
7. Mow, VC., Huiskes, R. Basic Orthopaedic Biomechanics and Mechanobiology. 3. Philadelphia: Lippincott Williams Wilkins; 2005.

8. Maroudas A. Physicochemical properties of cartilage in the light of ion exchange theory. Biophysical Journal. 1968; 8:575–595. [PubMed: 5699797]
9. Walker PS, Dowson D, Longfield MD, Wright V. “Boosted lubrication” in synovial joints by fluid entrapment and enrichment. Annals of the rheumatic diseases. 1968; 27:512–520. [PubMed: 5728097]
10. McCutchen CW. Mechanism of animal joints: Sponge-hydrostatic and weeping bearings. Nature. 1959; 184:1284–1285. [PubMed: 26219114]
11. Dowson D. Elastohydrodynamic and micro-elastohydrodynamic lubrication. Wear. 1995; 190:125–138.
12. Schmidt TA, Sah RL. Effect of synovial fluid on boundary lubrication of articular cartilage. Osteoarthritis and Cartilage. 2007; 15:35–47. [PubMed: 16859933]
13. Bonnevie ED, Galesso D, Secchieri C, Cohen I, Bonassar LJ. Elastoviscous Transitions of Articular Cartilage Reveal a Mechanism of Synergy between Lubricin and Hyaluronic Acid. Plos One. 2015; 10:e0143415. [PubMed: 26599797]
14. Gleghorn JP, Bonassar LJ. Lubrication mode analysis of articular cartilage using Stribeck surfaces. Journal of Biomechanics. 2008; 41:1910–1918. [PubMed: 18502429]
15. Lewis PR, McCutchen CW. Experimental evidence for weeping lubrication in mammalian joints. Nature. 1959; 184:1285. [PubMed: 14416552]
16. McCutchen CW. The frictional properties of animal joints. Wear. 1962; 5:1–17.
17. Krishnan R, Kopacz M, Ateshian GA. Experimental verification of the role of interstitial fluid pressurization in cartilage lubrication. Journal of Orthopaedic Research. 2004; 22:565–570. [PubMed: 15099636]
18. Carter MJ, Basalo IM, Ateshian GA. The temporal response of the friction coefficient of articular cartilage depends on the contact area. Journal of Biomechanics. 2007; 40:3257–3260. [PubMed: 17490673]
19. Kuo CK, Li WJ, Mauck RL, Tuan RS. Cartilage tissue engineering: its potential and uses. Current Opinion in Rheumatology. 2006; 18:64–73. [PubMed: 16344621]
20. Temenoff JS, Mikos AG. Review: tissue engineering for regeneration of articular cartilage. Biomaterials. 2000; 21:431–440. [PubMed: 10674807]
21. Hunziker EB, Lippuner K, Keel MJB, Shintani N. An educational review of cartilage repair: precepts & practice - myths & misconceptions - progress & prospects. Osteoarthritis and Cartilage. 2015; 23:334–350. [PubMed: 25534362]
22. Sakata R, Iwakura T, Reddi AH. Regeneration of Articular Cartilage Surface: Morphogens, Cells, and Extracellular Matrix Scaffolds. Tissue Engineering Part B-Reviews. 2015; 21:461–473. [PubMed: 25951707]
23. Makris EA, Gomoll AH, Malizos KN, Hu JC, Athanasiou KA. Repair and tissue engineering techniques for articular cartilage. Nature Reviews Rheumatology. 2015; 11:21–34. [PubMed: 25247412]
24. Sontjens SHM, Nettles DL, Carnahan MA, Setton LA, Grinstaff MW. Biodendrimer-based hydrogel scaffolds for cartilage tissue repair. Biomacromolecules. 2006; 7:310–316. [PubMed: 16398530]
25. Nettles DL, Vail TP, Morgan MT, Grinstaff MW, Setton LA. Photocrosslinkable hyaluronan as a scaffold for articular cartilage repair. Annals of Biomedical Engineering. 2004; 32:391–397. [PubMed: 15095813]
26. Degoricija L, Bansal PN, Sontjens SH, Joshi NS, Takahashi M, Snyder B, Grinstaff MW. Hydrogels for osteochondral repair based on photocrosslinkable carbamate dendrimers. Biomacromolecules. 2008; 9:2863–2872. [PubMed: 18800810]
27. Vilela CA, Correia C, Oliveira JM, Sousa RA, Espregueira-Mendes J, Reis RL. Cartilage Repair Using Hydrogels: A Critical Review of in Vivo Experimental Designs. Acs Biomaterials Science & Engineering. 2015; 1:726–739.
28. Nettles DL, Chilkoti A, Setton LA. Applications of elastin-like polypeptides in tissue engineering. Advanced Drug Delivery Reviews. 2010; 62:1479–1485. [PubMed: 20385185]
29. Wathier M, Lakin BA, Bansal PN, Stoddart SS, Snyder BD, Grinstaff MW. A Large-Molecular-Weight Polyanion, Synthesized via Ring-Opening Metathesis Polymerization, as a Lubricant for

Human Articular Cartilage. Journal of the American Chemical Society. 2013; 135:4930–4933. [PubMed: 23496043]

30. Samaroo KJ, Tan M, Putnam D, Bonassar LJ. Binding and lubrication of biomimetic boundary lubricants on articular cartilage. Journal of Orthopaedic Research. 2016; Epub ahead of print. doi: 10.1002/jor.23370
31. Lee SH, Shin H. Matrices and scaffolds for delivery of bioactive molecules in bone and cartilage tissue engineering. Advanced Drug Delivery Reviews. 2007; 59:339–359. [PubMed: 17499384]
32. Nazempour A, Van Wie BJ. Chondrocytes, Mesenchymal Stem Cells, and Their Combination in Articular Cartilage Regenerative Medicine. Annals of Biomedical Engineering. 2016; 44:1325–1354. [PubMed: 26987846]
33. Mamidi MK, Das AK, Zakaria Z, Bhonde R. Mesenchymal stromal cells for cartilage repair in osteoarthritis. Osteoarthritis and Cartilage. 2016; 24:1307–1316. [PubMed: 26973328]
34. Li KC, Hu YC. Cartilage Tissue Engineering: Recent Advances and Perspectives from Gene Regulation/Therapy. Advanced Healthcare Materials. 2015; 4:948–968. [PubMed: 25656682]
35. Basalo IP, Mauck RL, Kelly TAN, Nicoll SB, Chen FH, Hung CT, Ateshian GA. Cartilage interstitial fluid load support in unconfined compression following enzymatic digestion. Journal of Biomechanical Engineering-Transactions of the Asme. 2004; 126:779–786.
36. Cooper BG, Stewart RC, Burstein D, Snyder BD, Grinstaff MW. A Tissue-Penetrating Double Network Restores the Mechanical Properties of Degenerated Articular Cartilage. Angewandte Chemie-International Edition. 2016; 55:4226–4230. [PubMed: 26934682]
37. Lakin BA, Grasso DJ, Shah SS, Stewart RC, Bansal PN, Freedman JD, Grinstaff MW, Snyder BD. Cationic agent contrast-enhanced computed tomography imaging of cartilage correlates with the compressive modulus and coefficient of friction. Osteoarthritis and cartilage/OARS, Osteoarthritis Research Society. 2013; 21:60–68.
38. Park SH, Krishnan R, Nicoll SB, Ateshian GA. Cartilage interstitial fluid load support in unconfined compression. Journal of Biomechanics. 2003; 36:1785–1796. [PubMed: 14614932]
39. Soltz MA, Ateshian GA. Experimental verification and theoretical prediction of cartilage interstitial fluid pressurization at an impermeable contact interface in confined compression. Journal of Biomechanics. 1998; 31:927–934. [PubMed: 9840758]
40. Mow V, Kuei S, Lai W, Armstrong C. Biphasic creep and stress relaxation of articular cartilage in compression: theory and experiments. Journal of biomechanical engineering. 1980; 102:73–84. [PubMed: 7382457]
41. Ateshian GA, Wang HQ, Lai WM. The role of interstitial fluid pressurization and surface porosities on the boundary friction of articular cartilage. Journal of Tribology-Transactions of the Asme. 1998; 120:241–248.
42. Arokoski JPA, Jurvelin JS, Vaatainen U, Helminen HJ. Normal and pathological adaptations of articular cartilage to joint loading. Scandinavian Journal of Medicine & Science in Sports. 2000; 10:186–198. [PubMed: 10898262]
43. Borotikar BS, Sheehan FT. In vivo patellofemoral contact mechanics during active extension using a novel dynamic MRI-based methodology. Osteoarthritis and cartilage/OARS, Osteoarthritis Research Society. 2013; 21:1886–1894.
44. Basalo IM, Chen FH, Hung CT, Ateshian GA. Frictional response of bovine articular cartilage under creep loading following proteoglycan digestion with chondroitinase ABC. Journal of Biomechanical Engineering-Transactions of the Asme. 2006; 128:131–134.
45. Quinn TM, Grodzinsky AJ. Longitudinal modulus and hydraulic permeability of poly(methacrylic acid) gels - Effects of charge-density and solvent content. Macromolecules. 1993; 26:4332–4338.
46. Mow, VC., Huiskes, R. Basic Orthopaedic Biomechanics and Mechanobiology. 3. Philadelphia: Lippincott Williams Wilkins; 2005.
47. Mow VC, Holmes MH, Lai WM. Fluid transport and mechanical properties of articular cartilage: a review. Journal of Biomechanics. 1984; 17:377–394. [PubMed: 6376512]
48. Chen AC, Bae WC, Schinagl RM, Sah RL. Depth- and strain-dependent mechanical and electromechanical properties of full-thickness bovine articular cartilage in confined compression. Journal of Biomechanics. 2001; 34:1–12. [PubMed: 11425068]

49. Reynaud B, Quinn TM. Anisotropic hydraulic permeability in compressed articular cartilage. Journal of Biomechanics. 2006; 39:131–137. [PubMed: 16271597]

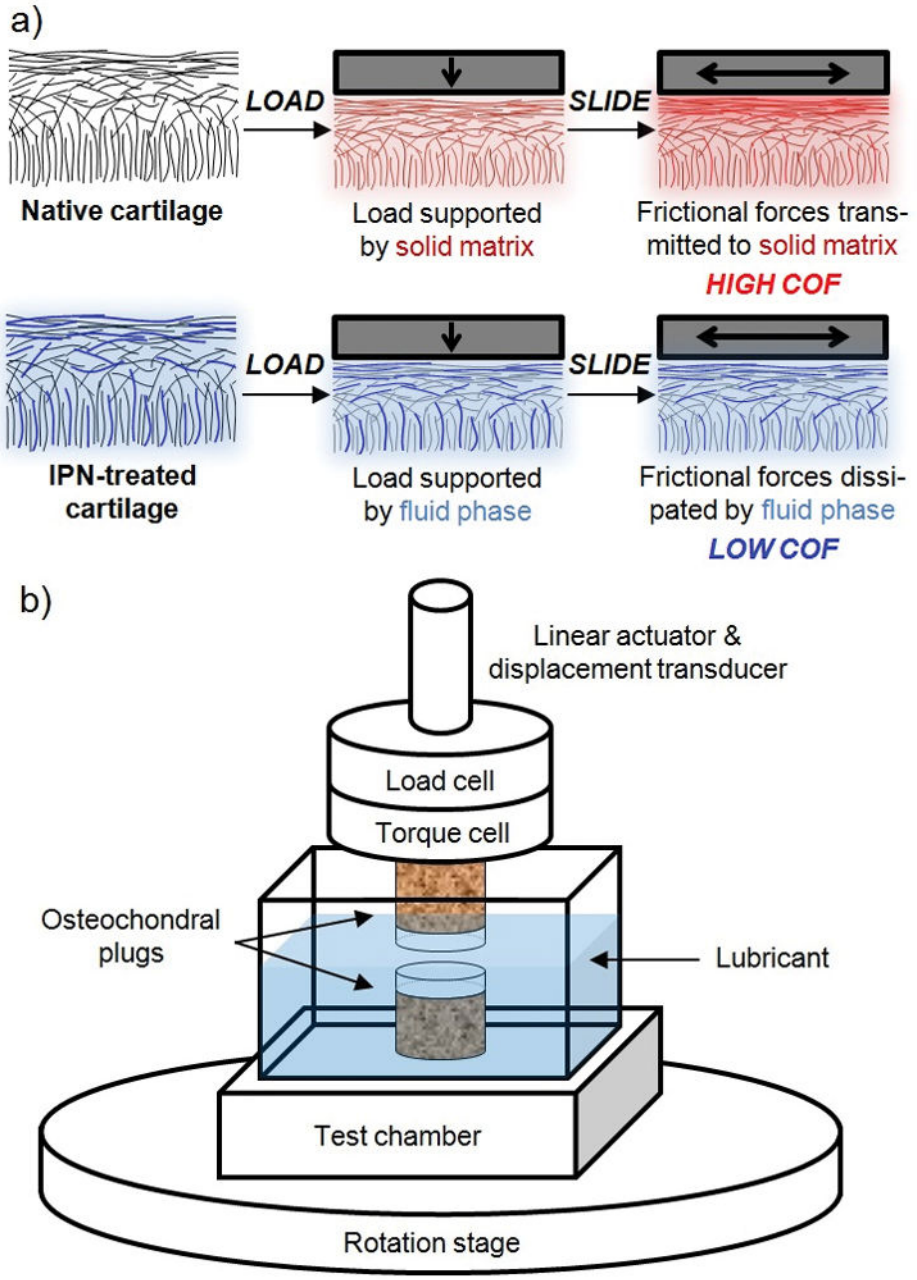

Figure 1.

(a) Relative to native cartilage, cartilage reinforced with an interpenetrating network (IPN-treated) allows a greater proportion of load support by the tissue's fluid phase (opposed to by solid matrix), in turn allowing sliding frictional forces to be dissipated through the fluid phase (opposed to the high solid-against-solid friction in non-treated tissue). (b) Schematic of friction testing configuration.

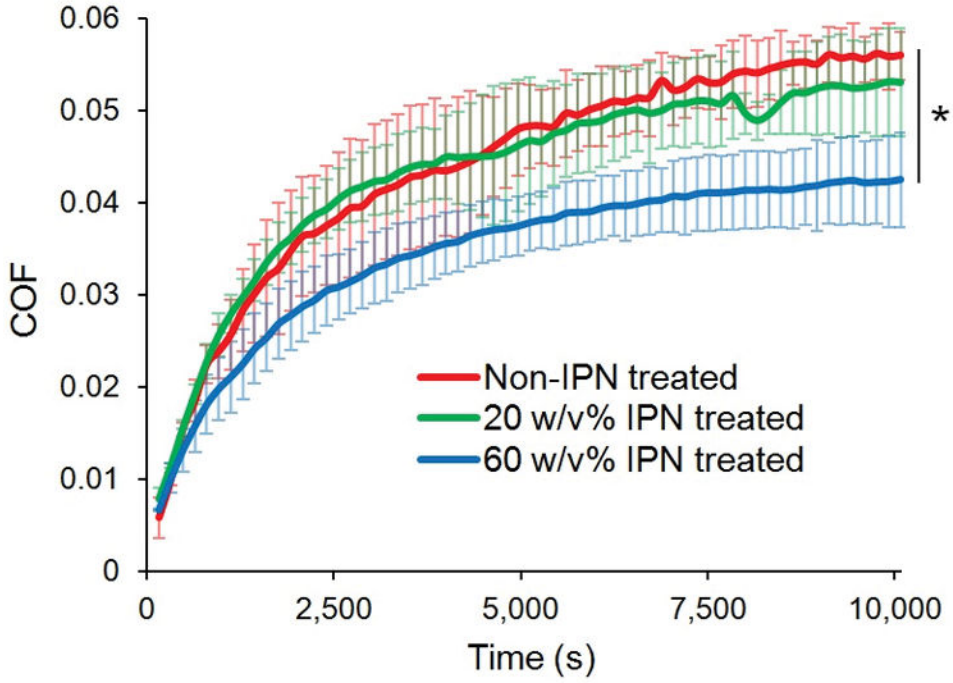

Figure 2.

COF as a function of time. Error bars represent standard deviations, N=3. * p = 0.015 comparing COF_{eq} of non-IPN treated vs 60 w/v% IPN treated cartilage.

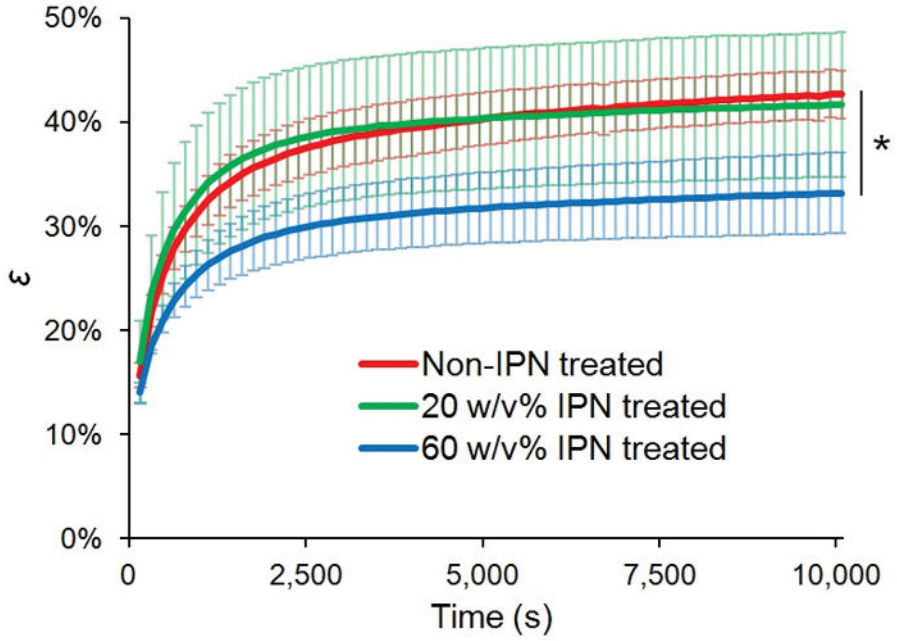

Figure 3.

Compressive engineering strain, ε, as a function of time. Error bars represent standard deviations, N=3. * p = 0.022 comparing ε_{eq} of non-IPN treated vs 60 w/v% IPN treated cartilage.

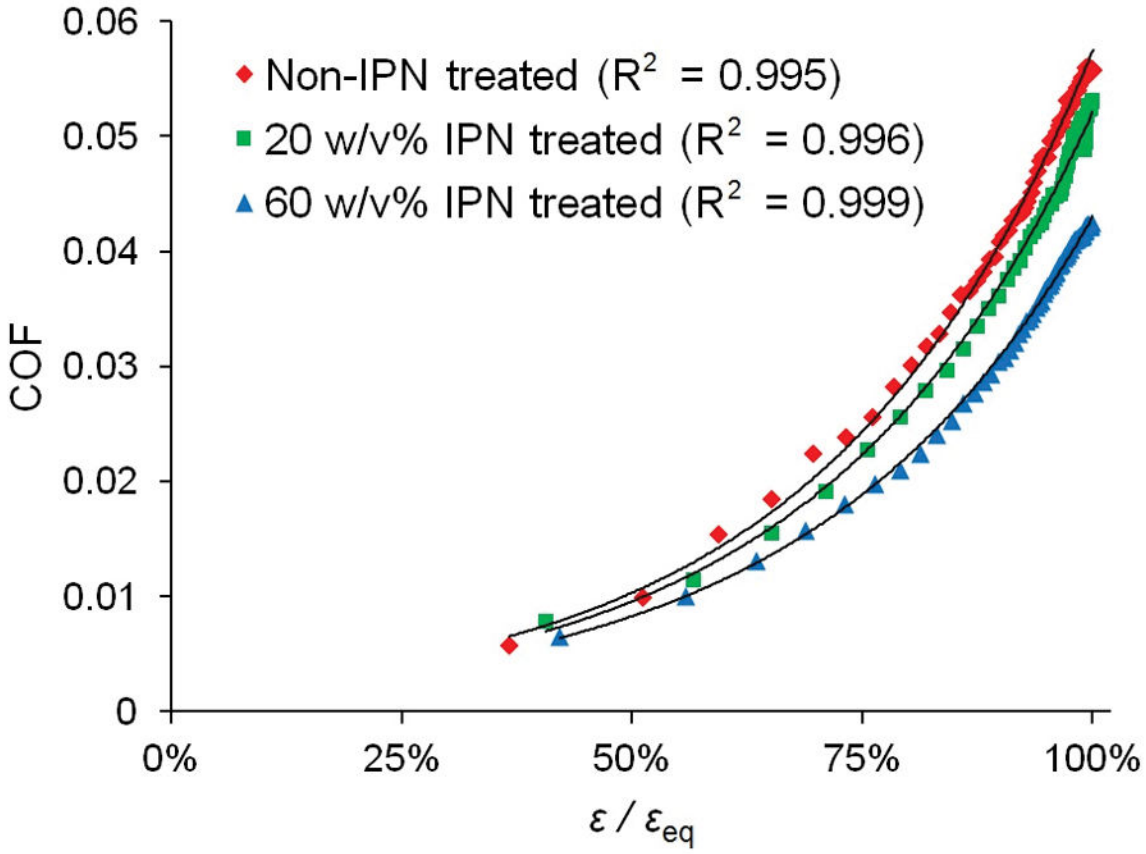

Figure 4.
COF as a function of $\varepsilon/\varepsilon_{eq}$, with least squares exponential regression curves. N=3, error bars omitted for clarity (see Supporting Information for plot containing error bars).

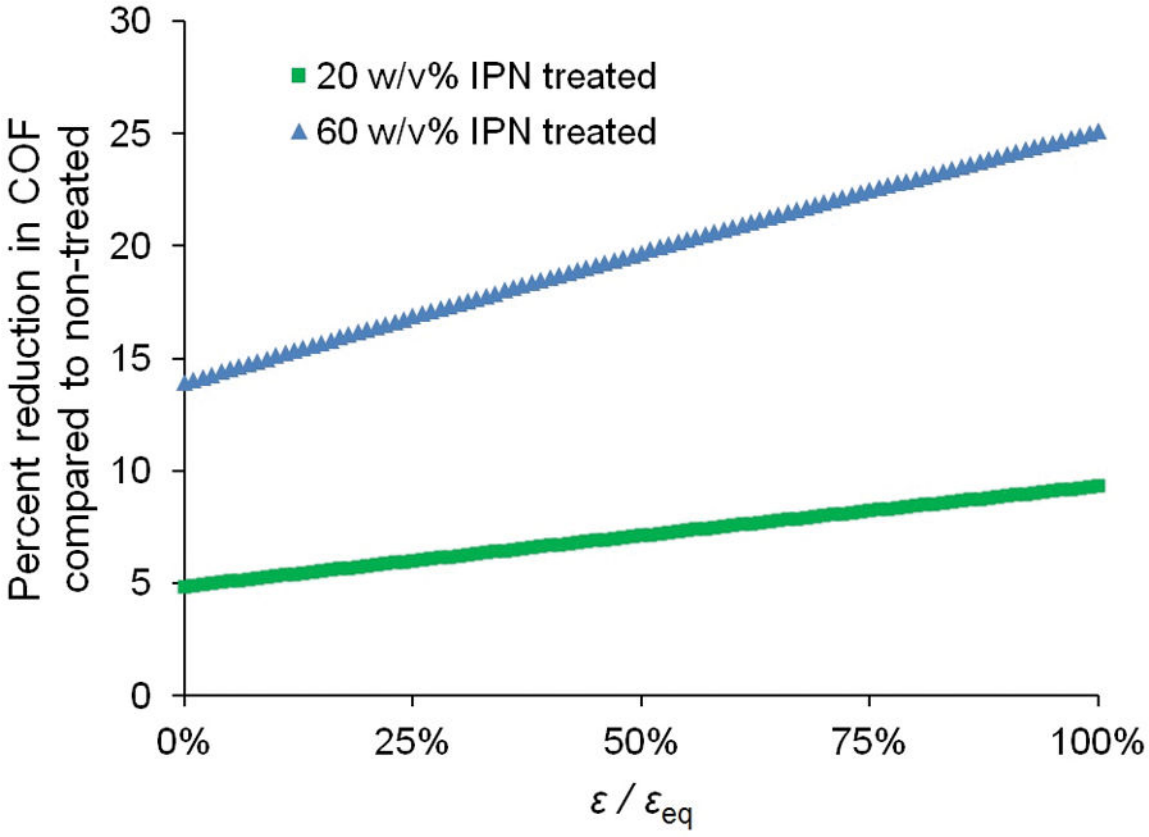

Figure 5.
Percent reduction in COF of 20 and 60 w/v% IPN treated cartilage compared to that of non-treated cartilage, as a function of $\varepsilon/\varepsilon_{eq}$.